

Shape-Independent Scaling of Excitonic Confinement in Realistic Quantum Wires

Original

Shape-Independent Scaling of Excitonic Confinement in Realistic Quantum Wires / Rossi, Fausto; Goldoni, G.; Molinari, E.. - In: PHYSICAL REVIEW LETTERS. - ISSN 0031-9007. - 78:18(1997), pp. 3527-3530.
[10.1103/PhysRevLett.78.3527]

Availability:

This version is available at: 11583/1405279 since:

Publisher:

APS American Physical Society

Published

DOI:10.1103/PhysRevLett.78.3527

Terms of use:

openAccess

This article is made available under terms and conditions as specified in the corresponding bibliographic description in the repository

Publisher copyright

(Article begins on next page)

Shape-Independent Scaling of Excitonic Confinement in Realistic Quantum Wires

Fausto Rossi, Guido Goldoni, and Elisa Molinari

Istituto Nazionale Fisica della Materia (INFM), and Dipartimento di Fisica, Università di Modena, I-41100 Modena, Italy

(Received 27 December 1996)

The scaling of exciton binding energy in semiconductor quantum wires is investigated theoretically through a nonvariational, fully three-dimensional approach for a wide set of realistic state-of-the-art structures. We find that in the strong confinement limit the same potential-to-kinetic energy ratio holds for quite different wire cross sections and compositions. As a consequence, a universal (shape- and composition-independent) parameter can be identified that governs the scaling of the binding energy with size. Previous indications that the shape of the wire cross section may have important effects on exciton binding are discussed in the light of the present results. [S0031-9007(97)03127-X]

PACS numbers: 73.20.Dx, 71.35.Cc, 78.66.Fd

The achievement of large exciton binding energies (E_b) is considered an important goal in the field of semiconductor nanostructures. On the one hand, large values of E_b are the result of the enhanced Coulomb coupling between electrons and holes due to their localization in the nanostructure and, therefore, they provide a clear fingerprint of low-dimensional confinement. On the other hand, large exciton binding energies are a prerequisite for exploiting excitonic nonlinearities in optical devices (e.g., switches and modulators) that can operate efficiently at room temperature.

For ideal two-dimensional (2D) systems, the binding energy of the ground-state exciton is 4 times the three-dimensional (3D) effective Rydberg. In quantum wells (QWs), E_b has been indeed observed to approach this limit when the well thickness is progressively reduced [1]. In the ideal one-dimensional (1D) limit E_b diverges [2], suggesting that exciton binding energies of quasi-1D (q1D) systems can be in principle increased by extreme quantum confinement much beyond the 2D limit [3]. Moreover, while for the Coulomb interaction the virial theorem limits E_b to just half of the potential (Coulomb) energy, the same limitation does not hold in the presence of an additional confining potential. In other words, if the only interactions are due to Coulomb forces, the virial theorem implies that the modulus of the ratio between average potential and kinetic energies is $\alpha = 2$; however, deviations from this condition are possible in q1D structures, and one might hope to obtain a more convenient ratio (i.e., larger α) by proper geometrical and compositional tailoring, thereby enhancing E_b .

Large exciton binding energies, clearly indicating additional confinement with respect to QWs of comparable confinement length L , have been indeed observed in artificial semiconductor wires fabricated by different techniques [4–9]. However, the dependence of E_b on the shape and height of the confining potential, and its scaling with size are still highly controversial. Based on theoretical predictions obtained through variational calculations for model wire geometries, the scaling of E_b is expected to be gov-

erned by the extension of the single-particle wave functions in the plane perpendicular to the free wire direction (which in most cases simply reflects the cross sectional area of the wire for a given barrier height), and to be much less sensitive to the shape of the wire [10]. On the experimental side, optical spectra have now been obtained for wires of different geometries. In particular, direct epitaxial overgrowth techniques on the cleaved edge of multi-QW samples [11] or on patterned substrates [12] have recently produced wires of good optical quality, with T-shaped and V-shaped cross sections, respectively. Among the recent experimental papers on such samples, some [4–6,9] essentially confirm the expected trends for the size dependence of E_b , while in others—T-shaped wires [7,8]—the values extracted for E_b are apparently much larger than expected on the basis of variational calculations [13,14].

The open question is whether for a specific shape of the wire cross section electron-hole Coulomb correlation is actually enhanced, due to effects that have been neglected in previous theoretical approaches. In this case, the parameters governing the scaling of exciton binding (if any) would have to be reconsidered. On the other hand, if this is not the case, one would still have to explain the inconsistencies between the values of E_b extracted from experimental data on different types of samples.

To address this problem, we make use of a theoretical approach recently proposed and used to study nonlinear optical spectra of quantum wires [15]. The scheme is based on a generalization of the well-known semiconductor Bloch equations (SBE) to the case of a multisubband wire structure. In this Letter, we focus on the quasiequilibrium regime where the solution of the SBE simply reduces to the solution of the polarization equation. This is performed by direct numerical evaluation of the polarization eigenvalues and eigenvectors, which fully determine the absorption spectrum. The main ingredients entering the calculation are the single-particle energies and wave functions, obtained numerically for an arbitrary 2D confinement potential which, e.g., can be deduced from TEM images of real samples, as in Ref. [6]. Since the proposed

approach is based on a full 3D multisubband description of the electron-hole Coulomb interaction [16], it allows a direct evaluation of the 3D exciton wave function, thereby eliminating any assumption on the form of the variational excitonic ground state, which would hamper the determination of possible shape effects.

The above approach has been applied to realistic V- and T-shaped quantum-wire (V-wire and T-wire) structures. For both geometries, two different sets of conduction and valence band offsets (V_e and V_h , respectively) have been considered, in order to simulate both low- x $\text{Al}_x\text{Ga}_{1-x}\text{As}$ and pure AlAs barrier compositions [17]. In total, we consider four sets of samples, which we label V1, V2, T1, T2, where V (T) refers to the wire shape, and 1 (2) refers to the low (high) barriers. For V-wires, we start from the reference-sample TEM profile of Ref. [6], and magnify or reduce both confinement directions by the same scale factor. Each sample is characterized by the confinement length L_V at the bottom of the V-shaped region. For T-wires, we consider a set of samples with different values of the parent QW width L_T , which includes the samples of Ref. [8] (here we only show data for T-wires with parent QWs of equal width). The wire geometries are sketched as insets in Fig. 1, and Table I summarizes the parameters characterizing the four quantum-wire sets reported in this Letter.

Figure 1 shows E_b and the corresponding mean potential energy $\langle V \rangle$ as a function of the characteristic size parameter of the wire, L_V or L_T . (Here and throughout the paper, the symbol $\langle \dots \rangle$ denotes the expectation value over the exciton ground state.) As expected, both binding and

potential energies increase with decreasing L_V or L_T ; for samples V2 and T2, corresponding to AlAs barriers, the excitonic binding is larger compared to the case of low-barrier samples V1 and T1.

Two important features result from Fig. 1. First, a given value of E_b corresponds to rather different values of L_V and L_T (note the different scale). This tells us that such size parameters are not adequate to characterize the actual exciton confinement. To introduce a more appropriate quantity, we define an effective exciton Bohr radius

$$a = \left\langle \frac{1}{r} \right\rangle^{-1}, \quad (1)$$

whose inverse is clearly proportional to the potential energy and, for a 3D bulk semiconductor, coincides with the usual exciton Bohr radius a_0 . The insets of Fig. 1 show a as a function of the relevant geometrical parameter, L_V or L_T . A same value of a corresponds to different values of L_V and L_T , with L_V always larger than L_T . Note that samples with similar binding energies correspond to similar values of a (see, e.g., the circled points, to be discussed below). The second feature resulting from Fig. 1 is that the ratio of binding to potential energy is rather constant (shape and barrier independent), and relatively close to one. This tells us that for all the samples considered the mean kinetic energy $\langle K \rangle$ is much smaller (about 4 times) than the potential energy.

Both features indicate a shape-independent scaling of the exciton binding energy. Indeed, by plotting the binding energy E_b of all samples vs the corresponding exciton

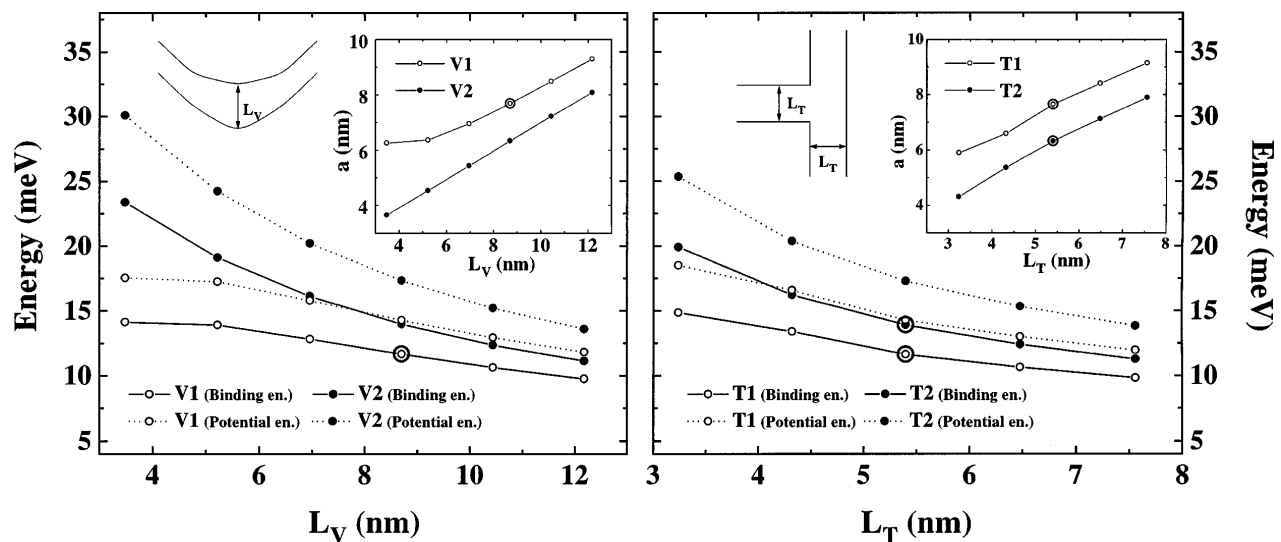


FIG. 1. Exciton binding energy E_b and mean potential energy $\langle V \rangle$ of V-wires (left) and T-wires (right) for the samples of Table I. Full dots indicate high barrier samples, and empty dots indicate low barrier samples, according to the legends. Full lines (E_b) and dotted lines ($\langle V \rangle$) are just guides to the eye. In the left insets we sketch the wire geometry, with indication of the relevant geometrical parameter. In the right insets we show the calculated effective exciton Bohr radius, a , vs the relevant geometrical parameter. The circled points refer to sample parameters corresponding to Ref. [6] (V-wires) and Ref. [8] (T-wires). For sample parameters see also Table I.

TABLE I. Sample parameters and calculated E_b for the four sets of wires. V_e , V_h , and E_b are given in meV; L_V , L_T are given in nm. Other parameters are the electron effective mass $m_e = 0.067m_0$, and the hole effective mass $m_h = 0.38m_0$ along the [001] crystallographic direction, and $m_h = 0.69m_0$ along the [110] crystallographic direction, where m_0 is the free electron mass. The values in boldface refer to samples for which E_b has been experimentally evaluated.

V1	V_e	150	L_V	3.48	5.22	6.96	8.70^a	10.44	12.18
	V_h	50	E_b	14.12	13.91	12.81	11.66	10.63	9.76
V2	V_e	1036	L_V	3.48	5.22	6.96	8.70	10.44	12.18
	V_h	558	E_b	23.37	19.10	16.13	13.97	12.36	11.12
T1	V_e	243	L_T	3.24	4.32	5.40^b	6.48	7.56	
	V_h	131	E_b	14.85	13.39	11.63	10.63	9.82	
T2	V_e	1036	L_T	3.24	4.32	5.40^b	6.48	7.56	
	V_h	558	E_b	19.90	16.23	13.90	12.41	11.26	
QW	V_e	1036	L	3.24	5.40	8.64	16.20		
	V_h	558	E_b	10.76	9.83	8.89	7.41		

^aParameters corresponding to the sample of Ref. [6].

^bParameters corresponding to the samples of Ref. [8].

radius a (Fig. 2), what we obtain is a universal (shape and barrier independent) curve, $E_b \sim \frac{1}{a}$. A universal scaling of the mean potential and kinetic energy [18] is apparent in the $\langle V \rangle$ vs $\langle K \rangle$ plot reported in the inset of Fig. 2; to a very good approximation, all sets of points for V-wires and T-wires fall on a straight line with slope α very close to 4. For comparison, we have performed analogous calculations for a set of QWs (the parameters are defined in Table I). As shown in Fig. 2, we find that E_b scales with a similarly to q1D structures, although with a different prefactor. If $\langle V \rangle$ is plotted vs $\langle K \rangle$ (inset of Fig. 2), in fact, the points for QWs again fall on a

straight line, but now the slope is $\alpha = 2$ within numerical accuracy.

We can therefore conclude that, for q1D structures in the strong-confinement regime considered here, the potential-to-kinetic energy ratio is still a constant. However, its value is found to be twice the value imposed by the conventional virial theorem in 3D and ideal 2D systems, which we find to be also followed by QWs of comparable confinement lengths. In this respect, our findings confirm that q1D confinement is indeed advantageous for the purpose of obtaining enhanced exciton binding, and provide a general and quantitative prescription for tailoring E_b by tuning the effective exciton Bohr radius a through the geometrical size parameters.

At the same time, however, the universal scaling law of Fig. 2 sets a clear limit for the possible effects of choosing different shapes of the wire cross section, as long as they correspond to similar values of the effective Bohr radius a . For a given value of a , there is no hope to further increase E_b by tailoring the potential-to-kinetic energy ratio α through the geometry of the confining profile.

This last conclusion is in apparent contradiction with some findings that have been reported recently, based on optical experiments on different wires. In particular, a very large enhancement of the exciton binding energy was recently reported in high-quality T-wires, with estimated E_b reaching values 6–7 times larger than the corresponding 3D effective Rydberg [8]. These values are much larger than our theoretical findings for the same nominal potential profile [19]. More importantly, the effective Bohr radius for such T-wire geometry is found to be very close to the value of a obtained for samples of different shape (V-wires, Ref. [6]), where much smaller values of E_b were reported [20]. Our calculated E_b for such V-wire and T-wire samples of comparable a (highlighted by circled points in Fig. 1 and boldface characters in Table I) are, of course, very similar. We think that the origin of this

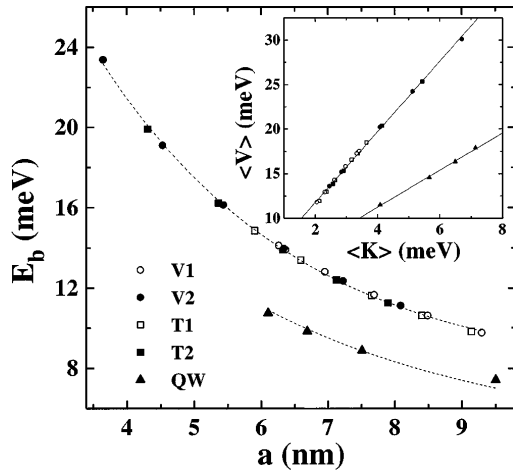


FIG. 2. Exciton binding energy E_b vs effective exciton Bohr radius, a , for the four sets of V-wires and T-wires, and for the set of QWs of Table I. Dashed curves are a fitting to $1/a$ form. The inset reports the average potential vs kinetic energy, falling on a straight line with slope $\alpha \approx 4$ for all wire samples. Results for QW structures are also shown for comparison; in this case $\alpha \approx 2$. Solid lines are a linear fit to the calculated points.

apparent discrepancy is in the procedure adopted in Ref. [8] to extract E_b from the experimental data. There, the measured quantity is the energy shift of the T-wire exciton with respect to the exciton of the parent QW, while E_b is derived by subtracting quantities that are estimated on the basis of simplified models. Among these, the largest approximation is made in the estimate of the energy shift between the lowest single-particle transitions of the T-wire and the parent QW: If we perform accurate calculations, including realistic masses and valence band mixing as described in Ref. [21], we find that the values used in Ref. [8] are largely underestimated [22], leading to an overestimated value of E_b . Further approximations pointed out by the authors (e.g., the indirect determination of L_T) may also contribute to an overestimation of E_b , but are probably less important. When these corrections are taken into account, the experimental data of Someya *et al.* [8] are indeed compatible with the present theoretical picture, as well as with the previous experimental results [6].

In summary, we have shown that in strongly confined quantum wires the average Coulomb and kinetic energies are proportional; their constant ratio is very close to 4, i.e., twice the conventional “virial” value—which holds in homogeneous systems and is found here to apply also to QWs—thus allowing enhanced E_b . As a consequence of this same proportionality, the scaling of E_b is found to be governed by a universal parameter that limits the possible differences due to variations in the shape of the wire cross section. Our results for realistic V-wires and T-wires in the strong confinement regime are consistent with the available experimental data and offer a guideline for tailoring binding energies in these structures.

We are grateful to T. Someya for useful discussions, and to T.L. Reinecke for useful correspondence and for communicating results prior to publication. This work was supported in part by the EC through the TMR-Network “Ultrafast.”

[1] See, e.g., G. Bastard, *Wave Mechanics Applied to Semiconductor Heterostructures* (Les Editions de Physique, Les Ulis, 1988), Chap. IV, and references therein.
 [2] R. Loudon, *Am. J. Phys.* **27**, 649 (1959); R.J. Elliot and R. Loudon, *J. Phys. Chem. Solids* **8**, 382 (1959); **15**, 196 (1960).
 [3] Tetsuo Ogawa and Toshihide Takagahara, *Phys. Rev. B* **43**, 14 325 (1991); **44**, 8138 (1991).
 [4] Y. Nagamune *et al.*, *Phys. Rev. Lett.* **69**, 2963 (1992).
 [5] W. Wegscheider *et al.*, *Phys. Rev. Lett.* **71**, 4071 (1993).
 [6] R. Rinaldi *et al.*, *Phys. Rev. Lett.* **73**, 2899 (1994).

[7] T. Someya, H. Akiyama, and H. Sakaki, *Phys. Rev. Lett.* **74**, 3664 (1995).
 [8] T. Someya, H. Akiyama, and H. Sakaki, *Phys. Rev. Lett.* **76**, 2965 (1996).
 [9] H. Weman *et al.*, *Phys. Rev. B* **53**, R6959 (1996), and references therein.
 [10] See, e.g., M.H. Degani and O. Hipolito, *Phys. Rev. B* **35**, 9345 (1987); P. Christol, P. Lefebvre, and H. Mathieu, *J. Appl. Phys.* **74**, 5626 (1993); P. Lefebvre, P. Christol, H. Mathieu, and S. Glutsch, *Phys. Rev. B* **52**, 5756 (1995).
 [11] L. Pfeiffer *et al.*, *Appl. Phys. Lett.* **56**, 1697 (1990).
 [12] E. Kapon *et al.*, *Phys. Rev. Lett.* **63**, 430 (1989).
 [13] Y.C. Chang, L.L. Chang, and L. Esaki, *Appl. Phys. Lett.* **47**, 1324 (1985).
 [14] T.L. Reinecke (private communication).
 [15] F. Rossi and E. Molinari, *Phys. Rev. Lett.* **76**, 3642 (1996); *Phys. Rev. B* **53**, 16462 (1996).
 [16] Note that the present multisubband approach includes on the same foot both confined and continuum states; in particular, this is essential in order to properly describe T-wires, where the 1D ground state is relatively close to the 2D continuum ensuing from the parent QWs.
 [17] For the V-wires of Ref. [6] the barriers are constituted by a short period AlAs/GaAs superlattice. This induces a rather shallow confinement which, from the point of view of the barrier height, is equivalent to a barrier made from a low- x $\text{Al}_x\text{Ga}_{1-x}\text{As}$ alloy.
 [18] The samples shown here are only a part of the full set of samples that we have investigated. We have performed similar calculations for T-wires with asymmetric parent QWs. We have also extended the numerical approach of Ref. [15] to include the polarization charge which forms at the interface between well and barrier materials due to dielectric mismatch. All the investigated samples fall on the same curves of Fig. 2.
 [19] A preliminary estimation of E_b in T-wires, reported in F. Rossi and E. Molinari, in *The Physics of Semiconductors*, edited by M. Scheffler and R. Zimmermann (World Scientific, Singapore, 1996), p. 1161, was affected by convergence inaccuracies, which resulted in a significant overestimation.
 [20] The same value of the effective exciton Bohr radius a is reached in V-wires and T-wires for different values of the size parameters: in general $L_V > L_T$. This is a consequence of the single-particle confinement, which we find to be stronger in V-wires than in T-wires when the barriers and the size parameters are taken to be the same ($L_V = L_T$).
 [21] G. Goldoni *et al.*, *Appl. Phys. Lett.* **69**, 2965 (1996); *Phys. Rev. B* **55**, 7110 (1997).
 [22] For sample S2 of Ref. [8], we calculate that the shift between the lowest single-particle transitions of the T-wire and the parent QW is underestimated by at least 8 meV. Indeed, in Ref. [8] the electron and hole confinement energies were estimated to be 20 and 1 meV, respectively. We find that the same quantities must be larger than 25 and 4 meV.